Chem. Res. Chin. Univ., 2018, 34(1), 138—144 doi: 10.1007/s40242-018-7173-7

Template Effect of Hydrophobically Associating Polymers on the Construction of Cuprous Oxide Micro Structure

DONG Lei[1], LIU Huan[1], LI Yanjuan[2], ZHANG Hongtao[1], YU Liangmin[1*] and JIA Lanni[3,4*]

1. Key Laboratory of Marine Chemistry Theory and Technology, Ministry of Education, College of Chemistry and Chemical Engineering, Ocean University of China, Qingdao 266100, P. R. China;

2. School of Chemistry and Chemical Engineering, Jiangsu Normal University, Xuzhou 221116, P. R. China;

3. National Engineering Research Center for Marine Drugs, Ocean University of China, Qingdao 266071, P. R. China;

4. Marine Biomedical Research Institute of Qingdao, Qingdao 266071, P. R. China

Abstract To determine the template effect of hydrophobically associating copolymers(HACPs) on the morphology of nano/micro structures, six HACPs were synthesized and used as templates to biomimetically synthesize cuprous oxide(Cu_2O), an important semiconductor. This experiment showed a clear relationship between the associating state of the HACP molecules and the morphology of the Cu_2O particles. Cu_2O hollow spheres were preferentially prepared when the HACP molecules were in an intramolecular associating state. Furthermore, a Cu_2O hexapod was easily obtained when the HACP molecules were in an intermolecular associating state. The morphologies of the Cu_2O crystals prepared in the presence of the HACPs also confirmed this result.

Keywords Template; Hydrophobically associating polymer; Cuprous oxide; Morphology

1 Introduction

Because of their excellent and special mechanical properties, natural biominerals, such as shell, bone and pearl layers have attracted great research interest. Studies have shown that biopolymers, such as proteins or polysaccharides, play a key role in the construction of those biominerals[1—3]. To biomimetically synthesize biominerals and nano/micro materials, many kinds of polymers, including natural large molecules and man-made polymers, have been successfully used as soft templates during the past three decades[4—7]. Hydrophobically associating copolymers(HACPs), which could assemble to micelles or solid network structures in water through hydrophobic association, played an important role as templates in micro/nano material biomimetic synthesis. Nanotubes[8], nanolines[9], nano particles[10], hollow spheres[11] and other materials with novel morphologies and performance characteristics have been prepared with the assistance of HACPs. However, many facts influencing the template effect of HACPs, such as the hydrophobically associating state of the HACP molecules, the structure of the hydrophobic monomer and the hydrophobic monomer content in the HACPs, have not yet been discussed.

Considering the consensus that the polymer template impacts the morphology of micro-nano crystals significantly, a substance that was prepared in the presence of the polymer template may play the role of a probe to discover the regular pattern of the polymer acting as the template. Cuprous oxide(Cu_2O), which is an important inorganic material[12—16], exhibits a rich and varied appearance[17]. Consequently, its preparation reaction was chosen as a probe reaction. Herein, HACPs containing different hydrophobic monomers and different hydrophobic monomer amounts were synthesized. Then, with the help of HACPs, Cu_2O hollow spheres and hexapods with different diameters were synthesized. This research showed that it was the associating state of the HACP molecules in solution that affected the morphology of HACPs template and consequently induced the construction of Cu_2O particles with different morphologies.

2 Experimental

Acrylate(SA), 2-acrylamide-2-methylpropanesulphonic acid(AMPS), sodium dodecyl sulfate(SDS), 2,2′-azobis-(2-methylpropionamidine) dihydrochloride(V50), copper sulfate($CuSO_4·5H_2O$), sodium hydroxide(NaOH), and glucose($C_6H_{12}O_6·H_2O$) were purchased from Tianjin Tianjiao Chem. Co.(Tianjin, China) and were of analytical grade. These reagents were used without further purification. Acrylamide(AM, Zibo Dongpu Chem. Co.) was recrystallized from acetone and stored in the dark until required. *N*-(2,3,4-Trimethoxy-benzyl) acrylamide(TMBA) and *N*-(4-hydroxy-3-methoxy-benzyl) acrylamide(HMBA) were synthesized according to the literature[18]. The structure of HACPs was investigated on a Fourier transform infrared spectrometer(FTIR, Thermo

*Corresponding authors. E-mail: yuyan@ouc.edu.cn; jialann@163.com

Received May 15, 2017; accepted September 6, 2017.

Supported by the National Natural Science Foundation of China(No.51102219) and the Fundamental Research Funds for the Central Universities of China(Nos.201113024, 41404010204).

Nicolet, AVATAR 380) and a proton nuclear magnetic resonance spectrometer(^{1}H NMR, Bruker, AVANCEIII600). The crystal structure of Cu_2O was characterized by X-ray diffraction(XRD, Ricoh, Bruker-AXS, with Cu $K\alpha$ radiation). The morphology and microstructure were examined on a field-emission scanning electron microscope(FESEM, Hitachi, S4800) and an atomic force microscope(AFM, Agilent, Agilent5400).

2.1 Synthesis and Characterization of HACPs

HACPs were prepared by micellar free radical copolymerization, which was similar to a previous report[19] except for the difference in composition and type of initiator. Copolymer acrylamide-co-2-acrylamide-2-methylpropanesulphonic acid (PAP) without the hydrophobic monomer was prepared for comparison under polymerization conditions identical to those for the HACPs(Table 1). The total monomer concentration in water was constant at 10%(mass fraction) in all the reactions.

HACPs were characterized by FTIR and ^{1}H NMR. The apparent viscosity of its solution was measured with a Brookfield DV-I+ viscometer at a shear rate of 6 s^{-1} at 25 °C. The critical association concentration(c^*) value could be determined according to the apparent viscosity[19]. The intrinsic viscosities [η] were measured with a 0.6 mm Ubbelohde capillary viscometer in a water bath at (30.0±0.1) °C through the dilution extrapolation method. The associating states of HACPs at different concentrations were observed on an atomic force microscope.

Table 1 Conditions for the synthesis and characteristics of HACPs

Copolymer	Feed molar ratio n(AM):n(NaAMPS):n(HMBA):n(TMBA):n(SA)	[SDS]/(mol·L^{-1})	N_H[a,c]	Initiator(%, molar fraction)	Yield of HACPs[c](%)	[η][b,c]/(L·g^{-1})	Critical association concentration[c]/(g·L^{-1})
PAPH-1	84:15:1:0:0	0.0335	3	0.55	87.2	0.307	6.2
PAPH-2	83:15:2:0:0	0.0335	5.3	0.55	84.7	0.320	5.7
PAPH-3	82:15:3:0:0	0.0335	8	0.55	85.3	0.301	3.9
PAPH-4	81:15:4:0:0	0.0335	11	0.55	80.5	0.298	3.0
PAPT-2	83:15:0:2:0	0.0335	5.3	0.55	85.8	0.332	3.3
PAPS-2	83:15:0:0:2	0.0335	5.3	0.55	90.3	0.386	2.5

a. N_H is the hydrophobic microblock length; *b*. [η] is the intrinsic viscosity of polymer; *c*. N_H, yield(%), [η] and critical association concentration(c^*) were measured and calculated in a way identical to a previous report[19].

2.2 Synthesis and Characterization of Cu_2O in the Presence of HACPs

In a typical procedure, 400 mL of NaOH(2 mol/L) solution containing a certain amount of HACPs was poured into 200 mL of $CuSO_4$(1 mol/L) solution at 20 °C under vigorous stirring, and blue particles were produced immediately. 5 min later, 44 mL of glucose(1 mol/L) water solution was added to the reaction system. Meanwhile, the reaction temperature was increased to 70 °C and maintained for 15 min under continuous stirring. The products were filtered and washed with deionized water and ethanol, and finally dried at 60 °C in vacuum. The above synthesized HACPs were chosen as templates to discuss the effect of HACPs on the morphology of Cu_2O. The results are summarized in Table 2.

Table 2 Synthesis conditions and resulting morphology of Cu_2O

Cu_2O	HACPs	Concentration of HACP/(g·L^{-1})	Cu_2O morphology and diameter
C1	PAPH-2	1	Hexapods(15—20 μm) coexisting with hollow microspheres(2—8 μm)
C2	PAPH-2	3	Hexapods(15—20 μm) coexisting with hollow microspheres(2—5 μm)
C3	PAPH-2	5	Hexapods, 5—9 μm
C4	PAPH-2	7	Hexapods, 7—10 μm
C5	PAPT-2	3	Hexapods, 3—7 μm
C6	PAPS-2	3	Hexapods, 8—12 μm
C7	PAPH-1	5	Hexapods(14—16 μm) coexisting with hollow microspheres(2—3 μm)
C8	PAPH-3	5	Hexapods, 2—5 μm
C9	PAPH-5/0.30	5	Hexapods, 5—10 μm
C10	No template	0	Hexapods, 7—20 μm

3 Results and Discussion

3.1 Structural and Property Characterization of HACPs

The FTIR spectra of PAPH-2, PAPT-2 and PAPS-2 are shown in Fig.1. The absorption peaks appearing at 1660(Fig.1 curve *a*), 1658(Fig.1 curve *b*) and 1450 cm^{-1}(Fig.1 curves *a*, *b*) are ascribed to the stretching vibration of benzene rings. Peaks at 3159 cm^{-1}(Fig.1 curves *a*, *b*) and 3195 cm^{-1}(Fig.1 cureve *b*) are assigned to the ═C—H vibrations of benzene. The bands at approximately 1200, 1115 and 1041 cm^{-1}(Fig.1 curves *a*—*c*) can be attributed to the stretching vibration of —S═O in —SO_3^{-1}. Bands at 3427 and 1660 cm^{-1} correspond to the stretching vibration of —N—H and —C═O, respectively. Peaks at approximately 2864, 2928 and 2781 cm^{-1} are ascribed to the stretching vibrations of —CH_3, —CH_2 and —CH, respectively. It could be preliminarily proposed that PAPH-2, PAPT-2 and PAPS-2 were achieved.

^{1}H NMR spectra of PAPH-2, PAPT-2 and PAPS-2 are shown in Fig.2. The characteristic peaks of the chemical shift are identified in Table 3. It shows that there are groups derived from the hydrophobic monomers SA, TMBA and HMBA in the HACPs. Thus, hydrophobic monomers have copolymerized with other monomers. The molar concentration of the

hydrophobic unit in the HACPs could be calculated according to the ratio of the integral area of resonance peak of —OCH_3 to that of —CH in the ^{1}H NMR spectrum[20,21]. Therefore, it can be calculated that the hydrophobic monomer molar fraction was 2% in PAPT-2, PAPH-2 and PAPS-2, which equalizes to the molar ratio of hydrophobic monomer in the total monomer added. This indicated that all the hydrophobic monomer was consumed during the polymerization. The FTIR and ^{1}H NMR characterization confirmed that PAPH-2, PAPT-2 and PAPS-2 were synthesized successfully. PAPH-1, PAPH-3 and PAPH-4 were prepared with the same method as PAPH-2 with varied HMBA.

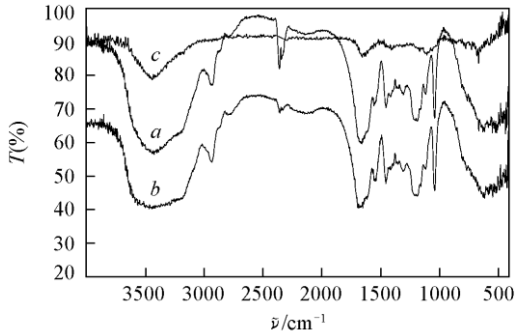

Fig.1 FTIR spectra of PAPT-2(*a*), PAPH-2(*b*), PAPS-2(*c*)

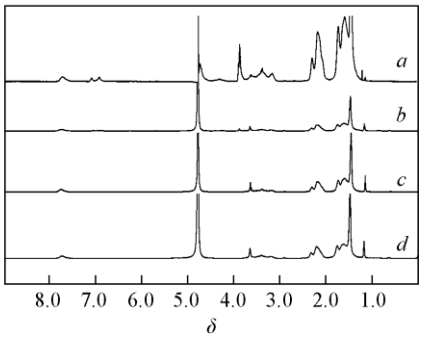

Fig.2 ^{1}H NMR spectra of PAPT-2(*a*), PAPH-2(*b*), PAPS-2(*c*) and PAP(*d*)

Solution: D_2O, —NH in TMBA or HMBA replaced by D atoms.

Table 3 Chemical shift value(δ) of HACPs for ^{1}H NMR spectra

Sample	δ							
	Benzene-H	—OCH_3 in TMBA or HMBA	—CH_2 in TMBA or HMBA	—CH_2 in chain	—CH in chain	—NH_2 in AM or —NH in NaAMPS	—CH_3 in NaAMPS	—CH_2 in NaAMPS
PAPT-2	6.62—7.15	3.87—3.90	4.32	1.5	2.24	4.77	1.69	3.42
PAPH-2	6.75—7.01	3.873	4.279	1.5	2.24	4.77	1.69	3.42
PAPS-2	—	—	—	1.5	2.24	4.77	1.69	3.42
PAP	—	—	—	1.5	2.24	4.77	1.69	3.42

3.2 Hydrophobic Association Capability of HACPs

c^* is used to show the hydrophobic association capability of the HACPs. The apparent viscosity variation with concentrations of the HACPs is shown in Fig.3. The c^* value could be derived according to the curves exemplified in Fig.4[22], and the values are listed in Table 1. The c^* values of the PAPHs show that the hydrophobic performance of the HACPs elevates with the increase of hydrophobic(HMBA) content in HACPs. This is due to the increase in hydrophobic content also increasing the length of the hydrophobic microblock. The c^* values of PAPH-2, PAPT-2 and PAPS-2, which employ HMBA, TMBA and SA as the hydrophobic monomers, respectively, decline successfully. This is attributed to the structure differences of the hydrophobic monomers(Fig.5). Both HMBA and TMBA

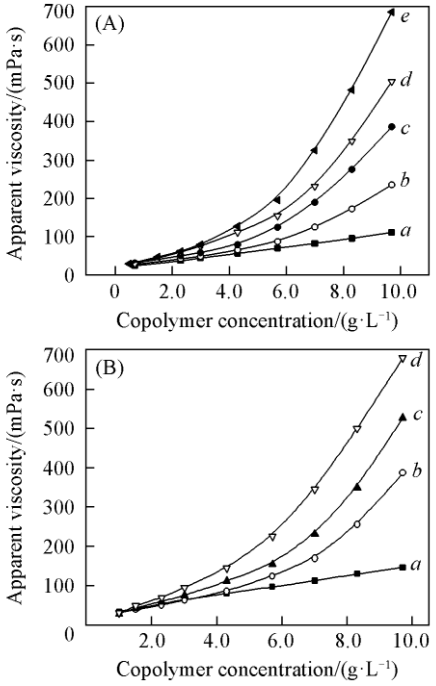

Fig.3 Apparent viscosity values of HACPs varying with different concentrations

(A) *a*. PAP; *b*. PAPH-1; *c*. PAPH-2; *d*. PAPH-3; *e*. PAPH-4. (B) *a*. PAP; *b*. PAPH-2; *c*. PAPT-2; *d*. PAPS-2.

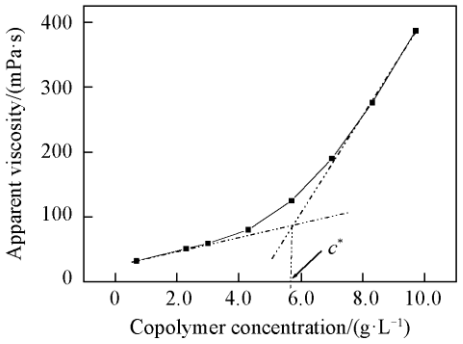

Fig.4 Diagram of calculating c^* value of PAPH-2 according to the curve of apparent viscosity with PAPH-2 concentration

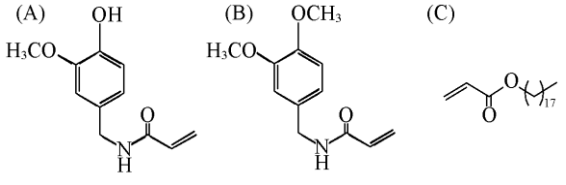

Fig.5 Molecular structure of HMBA(A), TMBA(B) and SA(C)

contain hydrophilic groups, such as methoxy group, which resulted in their hydrophobicity being lower than that of SA. The hydroxyl group in the benzene ring of HMBA that TMBA does not have further reduces the hydrophobicity of HMBA. In summary, the hydrophobic association capability declined with the decrease of the hydrophobic of the hydrophobic monomer.

3.3 Characterization of Cu_2O Synthesized in the Presence of HACPs

X-Ray scattering patterns of Cu_2O synthesized with different amounts of HACPs(PAPH-2) are shown in Fig.6.

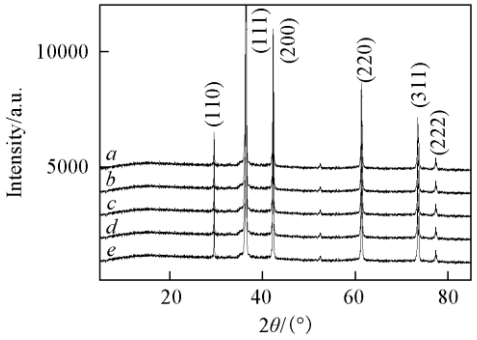

Fig.6 XRD patterns of Cu_2O prepared in the presence of PAPH-2 with different concentrations

Concentration of PAPH-2/(g·L^{-1}): *a*. 0; *b*. 1.0; *c*. 3.0; *d*. 5.0; *e*. 7.0.

Apparently, the peaks ascribed to cubic cuprite type Cu_2O (JCPDS No.05-0667) could be detected in all the samples, and no Cu and CuO peaks are observed, indicating that the presence of the PAPH-2 template did not impart the impurity to the final Cu_2O product. This conclusion also applies to the other HACPs as templates for the synthesis of Cu_2O.

3.4 Morphological Observation of Cu_2O and Template Mechanism of HACPs

The morphology of Cu_2O prepared with different concentrations of PAPH-2 was measured on a scanning electron microscope, as illustrated in Fig.7. It can be observed that most of the crystals are composed of hexapod and microsphere particles when the PAPH-2 concentration is lower than its c^*[Fig.7(A) and (B)], in which the microsphere is composed of rods. However, when the PAPH-2 concentration is near or larger than c^*, the Cu_2O microspheres disappear[Fig.7(C) and (D)]. The size of the Cu_2O short hexapods declines with increasing the PAPH-2 concentration. However, the size of Cu_2O synthesized at 7.0 g/L PAPH-2[Fig.7(E)] is slightly larger than that of Cu_2O prepared at 5.0 g/L PAPH-2[Fig.7(C)]. All these phenomena can be attributed to the associating state of the HACP molecules.

When the concentration of PAPH-2 was less than c^*, its hydrophobic chain blocks of PAPH-2 aggregated to microspheres through intramolecular association, and the hydrophilic chain segments strung the aggregates together. This made the PAPH-2 molecules resemble a string of pearls. Some hydrophilic chain segments were also around the aggregates to decrease the interfacial tension between the hydrophobic aggregates and water. Because of the shielding effect of sodium ions and copper ions in solution on carboxylic acid radicals, PAPH-2 molecular beads assembled to rod-shaped micelles and further self-assembled to hollow vesicles. Both of these assemblies are shown in Fig.8(A) and are consistent with the previous research[23—26]. Copper ions complexed by the carboxylic acid radicals on the surface of PAPH-2 vesicles were reduced to Cu_2O by glucose. Then, Cu_2O micro rods were achieved, induced by hydrophilic chain segments on the surface of HACP balls, and then covered the surface of the HACP vesicles. Cu_2O spheres with HACPs as their cores are observed [Fig.8(A)]. With the reduction of Cu^{2+}, HACP molecules previously fixed by Cu^{2+} re-dissolved to water across the shell of the Cu_2O microspheres; thus, Cu_2O hollow spheres were constructed. However, when the PAPH-2 concentration was lower than c^*, it was difficult to form enough vesicles for all Cu_2O to construct hollow spheres. Consequently, most Cu_2O particles formed short hexapods[Fig.7(A)], which were the same as those prepared under the same conditions but without HACPs.

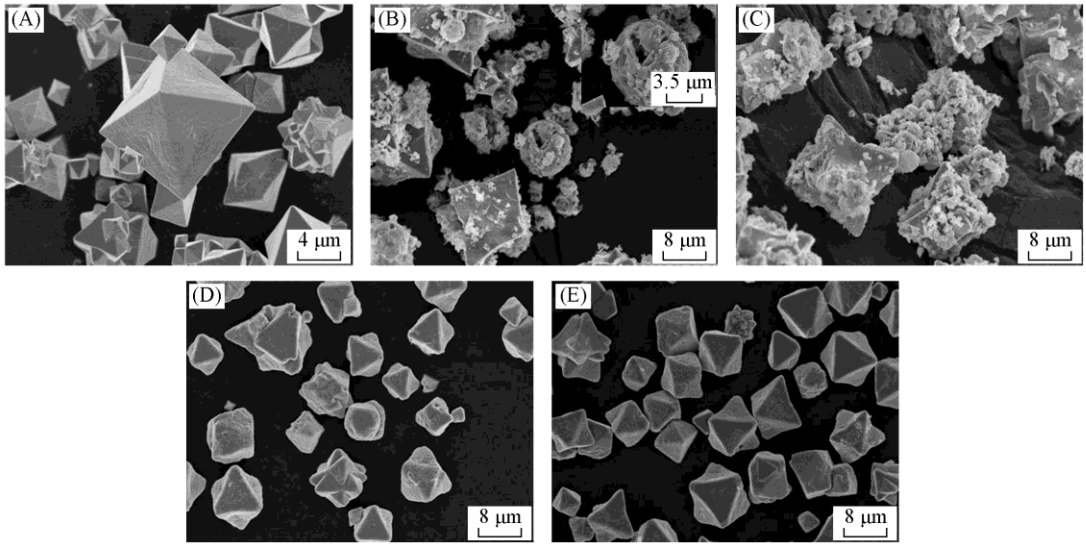

Fig.7 SEM images of Cu_2O prepared in the presence of PAPH-2 with different concentrations

Concentration of PAPH-2/(g·L^{-1}): (A) 0; (B) 1.0; (C) 3.0; (D) 5.0; (E) 7.0. Inset of (B): a more fine detail of Cu_2O microsphere.

When the concentration of PAPH-2 reached or slightly exceeded c^*, hollow vesicle assemblies of PAPH-2 molecules disappeared, and the PAPH-2 molecules formed an intermolecular solid network through intermolecular hydrophobic association[Fig.8(C) and (D)]. Then, hollow sphere Cu_2O particles disappeared[Fig.7(C) and (D)]. The unit cell of the PAPH-2 solid network could play the role of a micro reactor where Cu^{2+} had been reduced to a Cu_2O crystal. When the diameter of the Cu_2O crystal reached the size of the micro reactor, its growth would be restricted. Because of this, the diameter of the Cu_2O particles declined with the increasing PAPH-2 concentration[Fig.7(A)—(E)]. The size of Cu_2O particles prepared at 7.0 g/L PAPH-2[Fig.7(D)] is slightly larger than that prepared at 5.0 g/L PAPH-2[Fig.7(C)]. This may be attributed to the enlargement of the solid network unit with the increasing concentration of PAPH-2 higher than its c^* value. A similar phenomenon was previously reported[27]. AFM images of PAPH-2 [Fig.8(C) and (D)] show that the cell capacity of the solid network decreases with the increasing PAPH-2 concentration. This is due to the AFM measurement having the disadvantage of only showing the surface state of the sample but not the internal structure. Consequently, it was the associating state of the HACP template that determined the morphology of the Cu_2O.

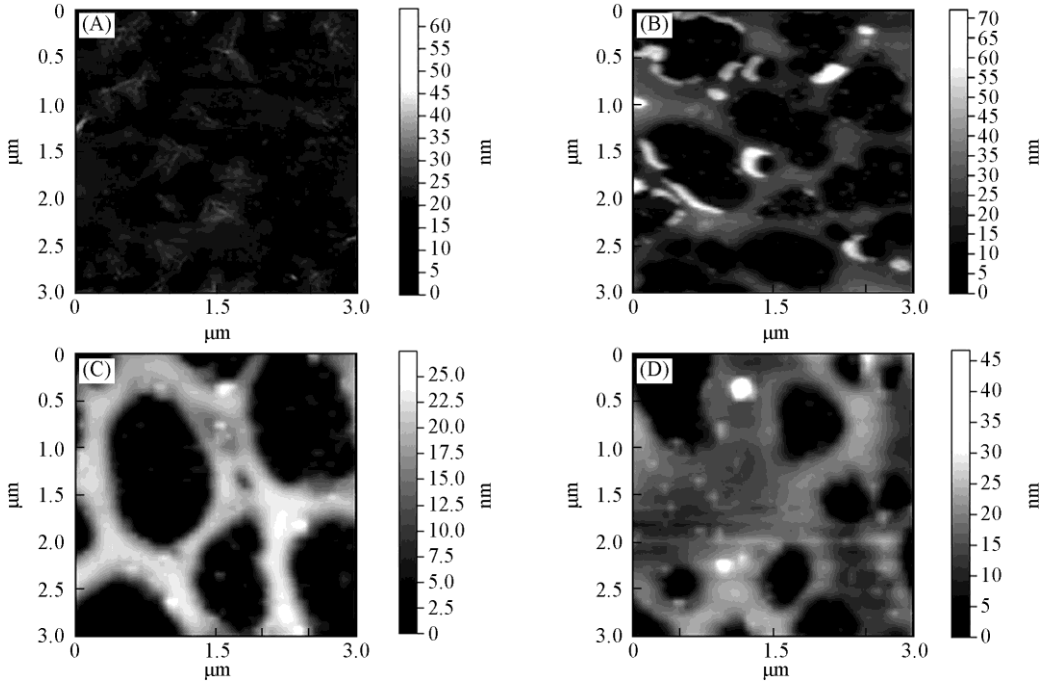

Fig.8 AFM images of PAPH-2 molecular with different concentrations

Concentration of PAPH-2/(g·L^{-1}): (A) 3.0; (B) 4.0; (C) 5.0; (D) 7.0.

To make sure that it was the associating state of the HACP template determining the morphology of the Cu_2O, PAPT-2 and PAPS-2, which contain different hydrophobic monomers, were used as templates to synthesize Cu_2O. SEM images of Cu_2O prepared with 3.0 g/L PAPH-2, PAPT-2 and PAPS-2, respectively, are shown in Fig.9. The morphologies of Cu_2O prepared in the presence of PAPH-2, PAPT-2 and PAPS-2[Fig.9(A)—(C)] are similar to that produced with 3.0, 5.0 and 7.0 g/L PAPH-2, respectively[Fig.7(C) and (D)]. This was induced by the differences of the hydrophobic association capabilities of PAPH-2, PAPT-2 and PAPS-2, as discussed above(Section 3.2). It is clear that they are in different hydrophobically associating states and assembled to diverse aggregates even though they are at the same concentration. Therefore, the PAPT-2 solution of 3.0 g/L, which is approximately equal to its c^* value(3.3 g/L, Table 1), is in an intermolecular hydrophobically associating state and constructed an intermolecular solid network. The PAPS-2 solution of 3.0 g/L, which is larger than its c^* value (2.5 g/L, Table 1) is in an intermolecular solid network state, while the unit capacity of its solid network is enlarged similar to that of the PAPH-2 solution of 7.0 g/L. PAPH-2(c^*, 5.7 g/L, Table 1) molecules with a concentration of 3.0 g/L are in an

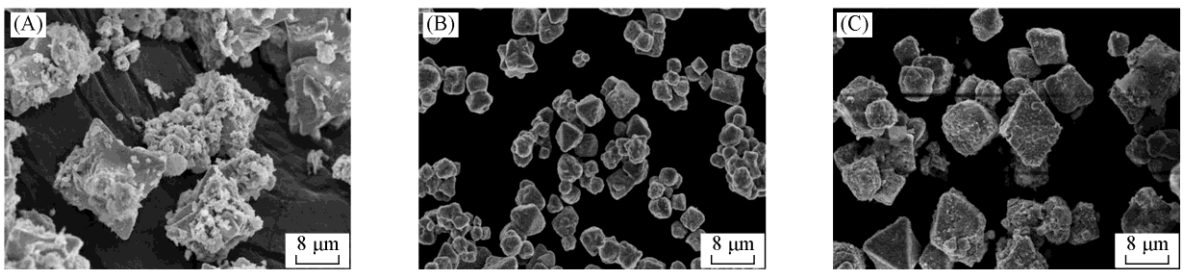

Fig.9 SEM images of Cu_2O prepared in the presence of HACPs containing different hydrophobic monomers(3.0 g/L)

Kind of hydrophobic monomer: (A) PAPH-2; (B) PAPT-2; (C) PAPS-2.

intramolecular associating state and assembled to micro rods and micelles. This implies that the hydrophobic associating state of HACPs as well as the hydrophobic monomer structure influences the morphology of Cu_2O directly.

To further confirm the above point, PAPH-1, PAPH-3 and PAPH-4 containing 1%, 3% and 4%(molar fraction) of the hydrophobic monomer HMBA were prepared and used as templates in preparing Cu_2O. The c^* values of PAPH-1, PAPH-3 and PAPH-4 are 6.2, 3.9 and 3.0 g/L(Table 1). When the HACP concentration is 5.0 g/L, the hydrophobic associating states of PAPH-1, PAPH-3 and PAPH-4 are intramolecular hydrophobic associating, intermolecular hydrophobic associating, and intermolecular hydrophobic associating but with enlarged unit cells, respectively. The hydrophobic associating states of these HACPs are the same as that of PAPH-2 with concentrations of 3.0, 5.0 and 7.0 g/L, respectively. The morphologies of the Cu_2O particles prepared in the presence of 5.0 g/L PAPH-1, PAPH-3 and PAPH-4 are shown in Fig.10. Their morphologies are similar to those of the particles produced with PAPH-2 at concentrations of 3.0, 5.0 and 7.0 g/L[Fig.7(C)—(E)], respectively. It is apparent that the associating state of the HACPs significantly influences the morphology of Cu_2O.

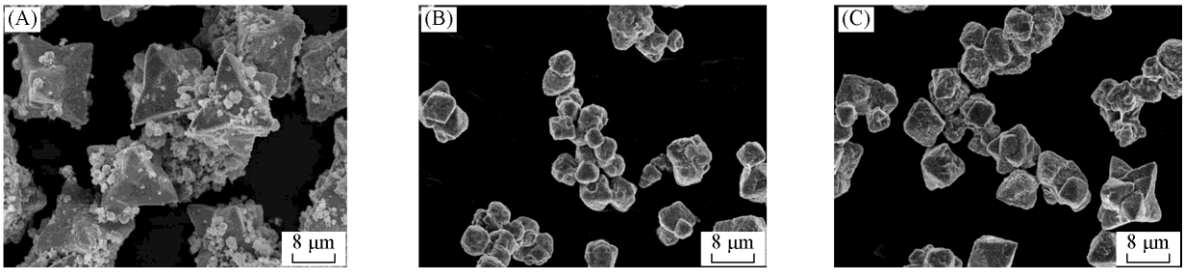

Fig.10 SEM images of Cu_2O prepared in the presence of HACPs containing different amounts of hydrophobic monomer

Hydrophobic monomer: (A) PAPH-1; (B) PAPH-3; (C) PAPH-4.

In conclusion, the structure and content of hydrophobic monomers change the c^* values of HACPs and then influence the morphology of Cu_2O indirectly. The associating state of the molecules is the direct factor that influences the templating effect of the HACPs. A possible schematic for the HACPs playing the role of template is shown in Fig.11.

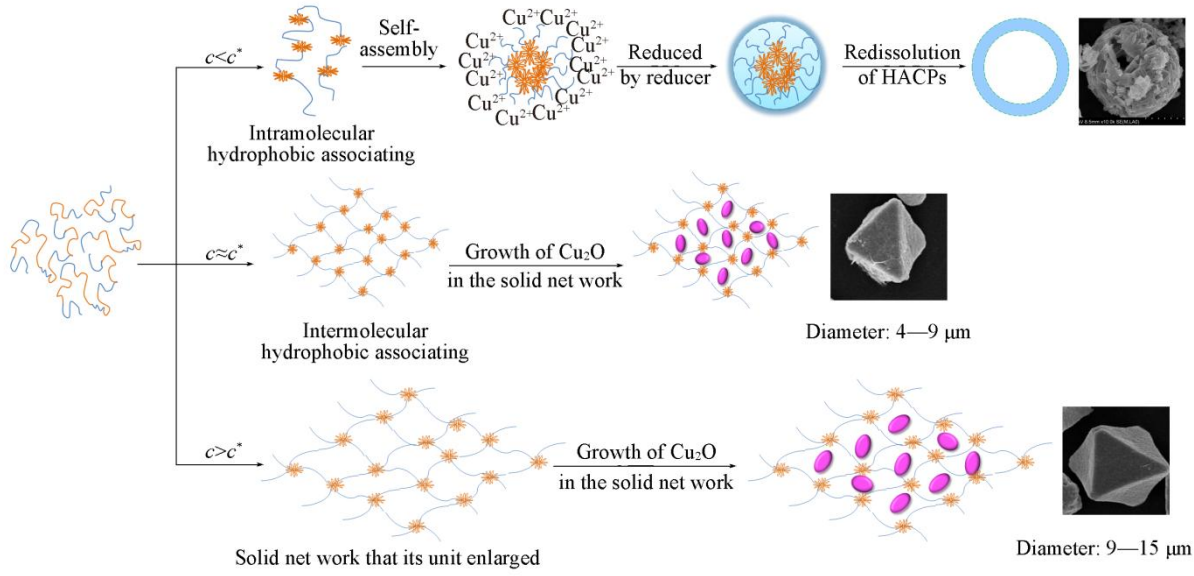

Fig.11 Schematic of HACPs playing the role of template in preparing Cu_2O

c^*: the critical association concentration of HACPs; c: the solution of HACPs in water.

4 Conclusions

HACPs can play the role of template in the biomimetic synthesis of some inorganic materials. The association state of HACPs determined the assembled form of HACP molecules and then caused the HACPs to exhibit different template effects. The structure and content of hydrophobic monomers in HACPs changed the c^* values of HACPs and then influenced the templating of HACPs indirectly. When the concentration of HACP in water was far less than its c^* value, the HACP molecules tended to aggregate to form hollow vesicles through intramolecular association. With the help of hollow vesicles, Cu_2O hollow spheres were preferentially prepared. When the concentration of HACP in water was approximately equal to its c^* value, a solid network of HACPs was constructed through intermolecular association, and micro Cu_2O hexapods were easily obtained. The unit cell of the HACPs solid network was enlarged when the concentration HACPs was far larger than its c^* value. Under these circumstances，Cu_2O hexapods with smaller diameters were easily obtained. These conclusions were confirmed by the morphologies of Cu_2O particles prepared in the presence of HACPs with different hydrophobic monomers

and those containing different amounts of hydrophobic monomers.

References

[1] Mnna S., *Nature*, **1993**, *365*(7), 499

[2] Weiner S., Addadi L., *J. Mater. Chem.*, **1997**, *7*(5), 689

[3] Annenkov V. V., Danilovtseva E. N., Pal'shin V. A., *RSC Adv.*, **2017**, *7*, 20995

[4] Hartgerink J. D., Beniash E., Stupp S. I., *Science*, **2001**, *294*(5547), 1684

[5] Zheng Z., Huang B., Ma H., *Cryst. Growth Des.*, **2007**, *7*(9), 1912

[6] Yan B. Q., Nan Z. D., Liu Y., *Chinese J. Chem.*, **2008**, *26*(12), 2302

[7] Finnemore A., Cunha P., Shean T., *Nat. Com.*, **2012**, *3*, 966

[8] Banerjee I. Yu A. L., Matsui H., *J. Am. Chem. Soc.*, **2003**, *125*(32), 9542

[9] Zhang D., Qi L., Ma J., Cheng H., *Chem. Mater.*, **2001**, *13*(9), 2753

[10] Qi L., Colfen H., Antonietti M., *Nano Lett.*, **2001**, *1*(2), 61

[11] Bastakoti B. P., Guragain S., Yokoyama Y., *Langmuir*, **2011**, *27*(1), 379

[12] Ng C. H. B., Fan W. Y., *J. Phys. Chem. B*, **2006**, *110*(42), 20801

[13] Du S. S., Cheng P. F., Sun P., Wang B., Cai Y. X., *Chem. Res. Chinese Universities*, **2014**, *30*(4), 661

[14] Poizot P., Laruelle S., Grugeon S., Dupont L., Taracon J. M., *Nature*, **2000**, *407*, 496

[15] Qiu X. Q., Miyauchi M., Sunada K., Minoshima M., *ACS Nano*, **2012**, *6*(2), 1609

[16] Chang Y., Teo J. J., Zeng H. C., *Langmuir*, **2005**, *21*(3), 1074

[17] Xu J. S., Xue D. F., *Acta. Mater.*, **2007**, *55*, 2397

[18] Yu L. M., An Z. G., Dong L., *Paint Coat. Ind.*, **2007**, *37*(7), 70

[19] Jia L. N., Yu L. M., Li R., *J. Appl. Polym. Sci.*, **2013**, *130*(3), 1794

[20] Feng Y. J., Billon L., Grassl B., *Polymer*, **2002**, *43*(7), 2055

[21] Pu H. T., Jiang W. C., Liu L., *Chem. J. Chinese Universities*, **2005**, *26*(9), 1743

[22] Gao B. J., Jiang L. D., Liu K. K., *Eur. Poly. J.*, **2007**, *43*(10), 4530

[23] Dobrynin A. V., Rubinstein M., *Macromolecules*, **1999**, *32*(3), 915

[24] Dobrynin A. V., Rubinstein M., *Macromolecules*, **2000**, *33*(21), 8097

[25] Zhang L., Eisenberg A., *Macromolecules*, **1999**, *32*, 2239

[26] Zhang L., Eisenberg A., *Polym. Adv. Technol.*, **1998**, *9*, 677

[27] Jiang L. F., Zhong C. R., Xu M., *Acta Phys.-Chim. Sin.*, **2010**, *26*(3), 535